Measurement 45 (2012) 311–316

Contents lists available at SciVerse ScienceDirect

Measurement

journal homepage: www.elsevier.com/locate/measurement

Investigation on residual stress and stress-optical coefficient for flexible electronics by photoelasticity

Y.C. Lee [a], T.S. Liu [a,*], C.I. Wu [b], W.Y. Lin [b]

[a] Department of Mechanical Engineering, National Chiao Tung University, Hsinchu 30010, Taiwan
[b] Center for Measurement Standards, Industrial Technology, Research Institute, Hsinchu 30042, Taiwan

ARTICLE INFO

Article history:
Received 2 May 2011
Received in revised form 17 November 2011
Accepted 21 November 2011
Available online 7 December 2011

Keywords:
Stress-optical coefficient
Residual stress
Photoelasticity
Thin film
Flexible electronics

ABSTRACT

For flexible electronics in manufacture, the full-field stress measurement is an important issue for the film deposited on the flexible substrate. In this work, the two-dimensional photoelasticity is proposed to measure stress-optical coefficients and an analytical derivation is carried out for investigation on full-field residual stresses under tensional forces. In experimental setup, a polarization beam splitter (PBS) is used to connect with two CCD cameras that are used to capture the intensity of right-hand and left-hand circular polarization separately. It has higher measured speed and better uniformity than a direct rotation method. Stress-optical coefficients can be calculated by extracting the slope from tensional stress versus optical retardation curve. Experimental results show that optical retardations for indium-tin-oxide (ITO)-coated PET (polyethylene terephthalate) substrates can be affected more easily than PET substrates under tensional forces. The difference of stress-optical coefficients between 0° and 90° orientations for PEN (polyethylene naphthalate) substrates is smaller than that for PET substrates. Furthermore, it shows residual stresses for ITO-coated PET substrates in 0° and 90° orientations are different under tensional stress.

1. Introduction

Flexible electronic devices are under development in modern technology. One of applications is "flexible display", which can be used as next generation monitors and replace newspaper and books in daily life in the form of electronic paper and electronic books. In flexible electronics, the flexibility depends on the substrate. Three kinds of substrates are considered to be flexible: thin glass, metal foil, and plastic. Plastic is the key material of choice, as it allows reasonable tradeoffs in mechanical, optical, and chemical performance. It is an inexpensive and useful material for in-line production via roll-to-roll (RTR) processes.

Polymers are very promising materials for flexible electrics with many advantages. They are transparent, light in weight, flexible, and robust. Polymers are a good alternative to the glass substrates that have been actively used for flat panel displays such as liquid crystal displays (LCDs) and plasma discharge panels (PDPs) [1].

Conventionally, indium-tin-oxide (ITO)-coated plastic substrates are used as the flexible conductive substrates, and have been studied intensively. Usually the stress will bend the flexible substrate, and may cause the crack or wrinkle for the film in some cases. The bending test from film deposition on the substrate is always an important problem during research [2,3]. Thin films on a substrate are usually in a stressed state. A convenient method to study stress in thin films is to deposit these films on a flat substrate and observe the curvature of the substrate due to the stress in the film. The Stoney equation relates the curvature of the substrate to the stress in the film [4]. Many researches for applications [5–8] and modifying the Stoney equation are investigated [9,10].

* Corresponding author. Tel.: +886 3 5712121x55123; fax: +886 3 5720634.
E-mail address: tsliu@mail.nctu.edu.tw (T.S. Liu).

0263-2241/$ - see front matter © 2011 Elsevier Ltd. All rights reserved.
doi:10.1016/j.measurement.2011.11.017

Typically, the film stress is measured from the change of curvature of substrate before and after deposition, and then uses the Stoney equation to calculate the quantity of the stress. Since the Stoney equation is an approximate equation and it can only get the average stress of the whole substrate, the photoelasticity is another method suitable for measuring the full-field stress. Photoelasticity is an experimental method for analyzing stress or strain field in mechanics. Optical methods in experimental stress analysis such as photoelasticity or thermoelasticity provide full-field information that relates stress distribution in a specimen or on a specimen surface [11]. Digital photoelasticity is a full-field technique, which provides information on principal stress difference (isochromatics) and the orientation of principal stress direction (isoclinics) at every pixel in the domain based on image processing [12]. The technique has been found to be quite useful for evaluating assembly stresses, residual stresses and contact stresses [13,14]. For obtaining isoclinic and isochromatic parameters, many techniques such as reflection photoelasticity [15] and interferometric photoelasticity [16] are reported in the literature for correcting the ambiguity and measuring stress components.

Digital photoelasticity measures optical retardations of the substrate before and after deposition, and then calculates the quantity of the stress by using the photoelastic equation. It can get the distribution of the stress for the whole substrate, and it is helpful for locating the influence of the stress. Since flexible substrates represent a fundamental component in the flexible electrics, the determination of stress-optical coefficients for substrates will help display design for stress analysis [17,18]. In this research, a two-dimensional photoelasticity is proposed by using a polarization beam splitter (PBS) connecting with two CCD cameras that are used to capture the separate intensity of right-hand and left-hand circular polarization at the same time. In addition, an analytical model has been presented for calculating full-field residual stresses under tensional forces. Stress-optical coefficients of polyethylene terephthalate (PET), polyethylene naphthalate (PEN) substrates and ITO-coated PET substrates are measured and residual stresses caused by ITO thin films for ITO-coated PET substrates are investigated under different amounts of tensional forces.

2. Optical birefringence effect

Fig. 1a and b show the schematic diagram and photo of the experimental setup of two-dimensional photoelasticity. Based on optical birefringence effects, the two-dimensional image data obtained in the experiment is used to

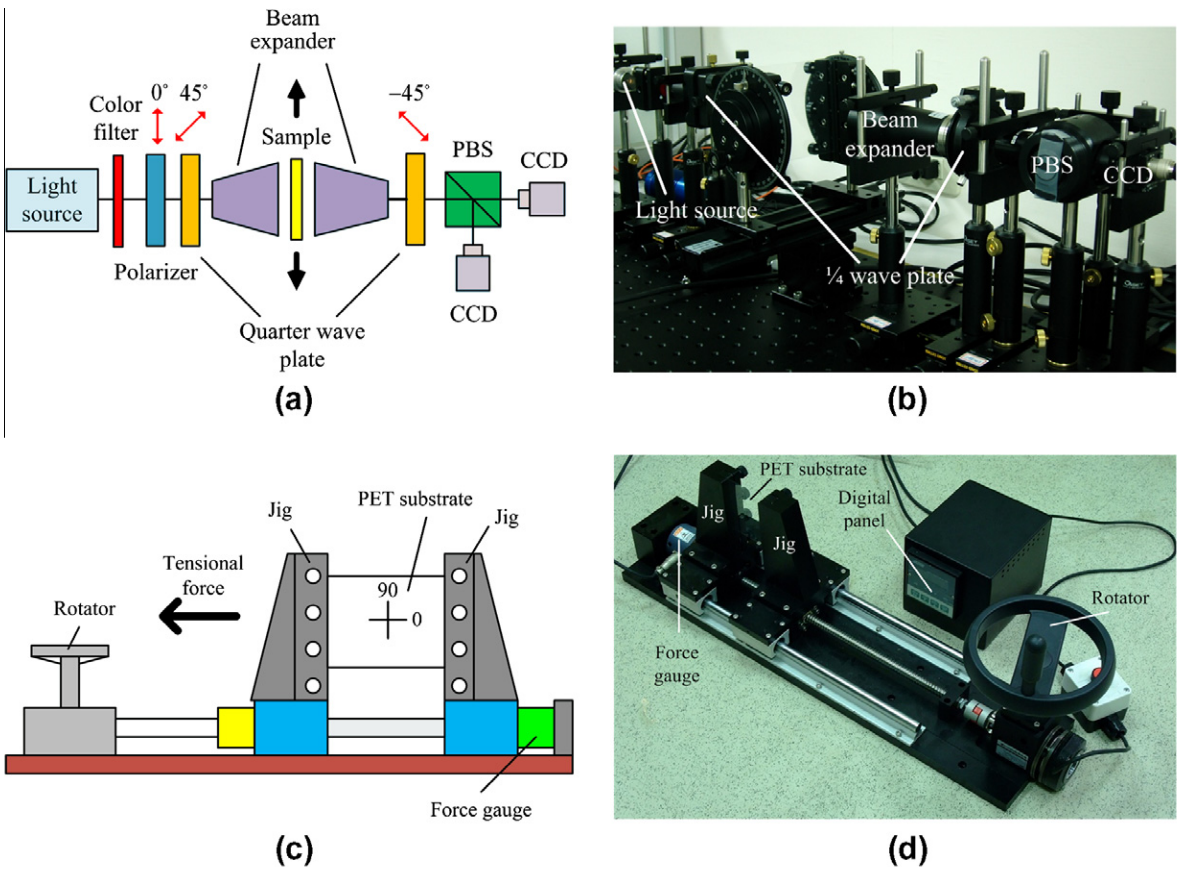

Fig. 1. (a) Schematic diagram and (b) photo of two-dimensional photoelastic measurement. (c) Schematic diagram and (d) photo of tensile testing machine.

illustrate the optical phase retardation by digital image processing techniques.

Birefringence is a photoelastic effect often used to analyze stresses in isotropic optical materials. For a birefringent material, because reflective index n has a directional dependence, the propagation velocity of light also has a directional dependence. It is a direct measure of the refractive index difference between two orthogonal axes in a plane perpendicular to the beam path axis. Let the state of stresses at a point be characterized by principal stresses σ_x, σ_y along the x and y directions. For a light beam propagating through a material along the z direction, the retardation δ can be defined as [17]

$$\delta = \frac{2\pi d}{\lambda}(n_x - n_y) = Cd(\sigma_x - \sigma_y) \tag{1}$$

where λ is wavelength of light, d is the thickness of the substrate, C is the stress-optical coefficient for the material, and n_x and n_y are the refractive indices seen by light when polarized in the x and y directions, respectively. The stress-optical coefficient is both material and wavelength dependent and defines the amount of the retardation produced per unit stress for light traveling through the material.

When thin films are deposited on the substrates, it will produce residual stresses due to the lattice misfit between films and substrates. The retardation δ_1 for bare substrates can be defined by Eq. (1) as

$$\delta_1 = C_1 d(\Delta\sigma) \tag{2}$$

where $\Delta\sigma$ is the uniaxial tensional stress and C_1 is the stress-optical coefficient of bare substrates. When thin films are deposited on substrates, the stress state changes due to mechanical properties of thin films. If the thickness of the thin film is very small, the retardation δ_2 changed under tensional stresses can be expressed as

$$\delta_2 = C_1 d(\Delta\sigma + \sigma') \tag{3}$$

where σ' is the residual stress between thin films and substrates. Substituting Eq. (2) into Eq. (3) gives the stress component σ'

$$\sigma' = (\delta_2 - \delta_1)/C_1 d \tag{4}$$

3. Photoelastic analysis

A two-dimensional measurement is quite different from a point measurement. The most significant difference lies in the fact that system nonuniformity is an inevitable problem for a two-dimensional measurement. A two-dimensional photoelastic measurement system consists of the following three parts: (1) an expanded light beam for illumination, (2) a tensile testing machine, and (3) two charge-coupled devices (CCD) cameras for two-dimensional optical-to-electrical image conversion and retardation calculation as shown in Fig. 1a and b. Fig. 1c and d shows the schematic diagram and photo of a tensile testing machine. A 125 μm thick PET substrate subjected to a tensional force in the 0° orientation is hold by two jigs. The 90° orientation is in the orthogonal direction of 0°. A tensional force is exerted by using a rotator and measured by a force gauge.

The collimated white light source passes through the 670 nm band pass filter with a 10 nm bandwidth to form a nearly monochromatic beam. Then the beam passes through a linear polarizer and a quarter wave plate to form a right-hand circular polarization beam before emitted into a beam expander. After passed through the sample, a quarter wave plate and a polarization beam splitter (PBS) connect with two CCD cameras that are used to capture the intensity of right-hand and left-hand circular polarization separately.

In a two-dimensional birefringence measurement system using the photoelastic effect, the uniformity by using a two-beam separation method is better than a direct rotation method. A PBS is used to separate incident light into P and S waves as shown in Fig. 1. The two-beam measurement has higher measured speed than a direct rotation method. It assumes that the specimen has a distribution of optical retardation magnitudes $\delta(x,y)$. The optical intensities of emitted P and S waves after image correction can be calculated by Jones matrices can be expressed as

$$I_P(x,y) = I_0 \sin^2(\delta(x,y)/2) \tag{5}$$

$$I_S(x,y) = I_0 \cos^2(\delta(x,y)/2) \tag{6}$$

where I_0 accounts for the amplitude of the incident light vector. Thus, the optical retardation image distribution can be expressed as

$$\delta(x,y) = \frac{180}{\pi}\left(2 \times \sin^{-1}\left(\sqrt{I_P(x,y)/(I_S(x,y)+I_P(x,y))}\right)\right) \tag{7}$$

where

$$I_S(x,y) + I_P(x,y) \neq 0 \tag{8}$$

Having solved Eq. (7), one can obtain the optical retardation image distribution $\delta(x,y)$.

4. Stress-optical coefficient measurement

Structures of polymer substrates have been developed for the flexible display due to their flexibility. Two different polymer substrates, 125 μm thick PET (Kimoto Films) and 125 μm thick PEN (Teonex Q83, Teijin DuPont Films) substrates are selected. In addition, 125 μm thick PET substrates with 50 nm thick ITO films on it are used to compare with PET and PEN substrates. Material properties of PET, PEN, and ITO are given in Table 1. These substrates are 100 mm in length and 100 mm in width. The optical intensities I_P and I_S for PEN substrates under tensional forces 0 kg and 27.01 kg in the 0-degree orientation are shown in Fig. 2a–d, respectively. The optical retardation image distributions calculated for PEN substrates under tensional forces 0 kg and 27.01 kg in the 0° orientation

Table 1
Material properties of PET, PEN, and ITO.

Material	Young's modulus (GPa)	Poisson's ratio
PET	4	0.3
PEN	5	0.3
ITO	118	0.2

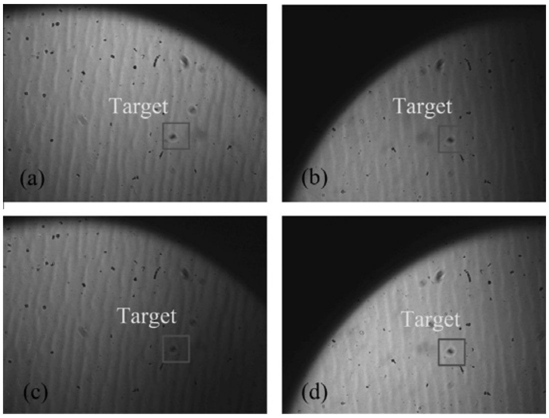

Fig. 2. Optical intensity of emitted (a) S wave and (b) P wave under tensional force 0 kg and (c) S wave and (d) P wave under tensional force 27.01 kg for PEN substrate.

are shown in Fig. 3a and b, respectively. Figs. 2 and 3 show that the optical retardation distribution is not uniform in the PET substrate by two-dimensional photoelastic measurement. Feature points in the center of measured blocks in Fig. 3a and b are selected for calculating stress-optical coefficients under different amounts of tensional forces.

Optical retardations of these substrates with 50 ∗ 50 pixels average are measured by increasing and decreasing applied tensional forces. Fig. 4a and b depict plots of stress versus optical retardation under increasing and decreasing

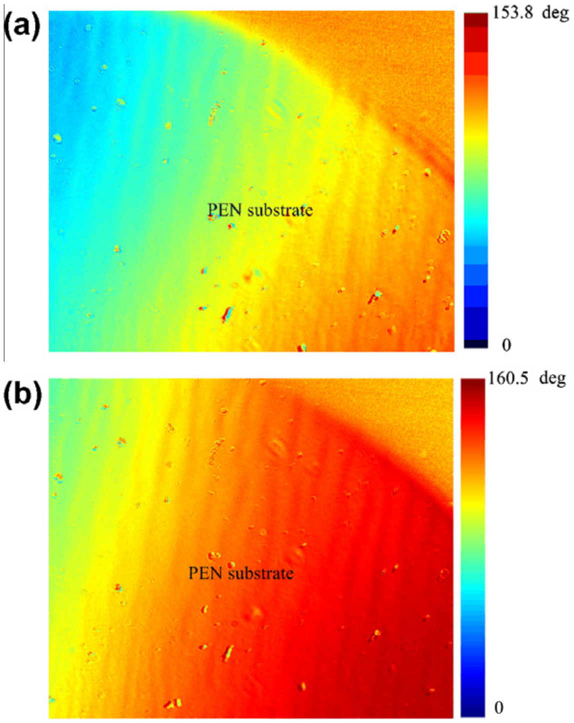

Fig. 3. Optical retardation image distributions for PEN substrates under tensional forces (a) 0 and (b) 27.01 kg in the 0° orientation.

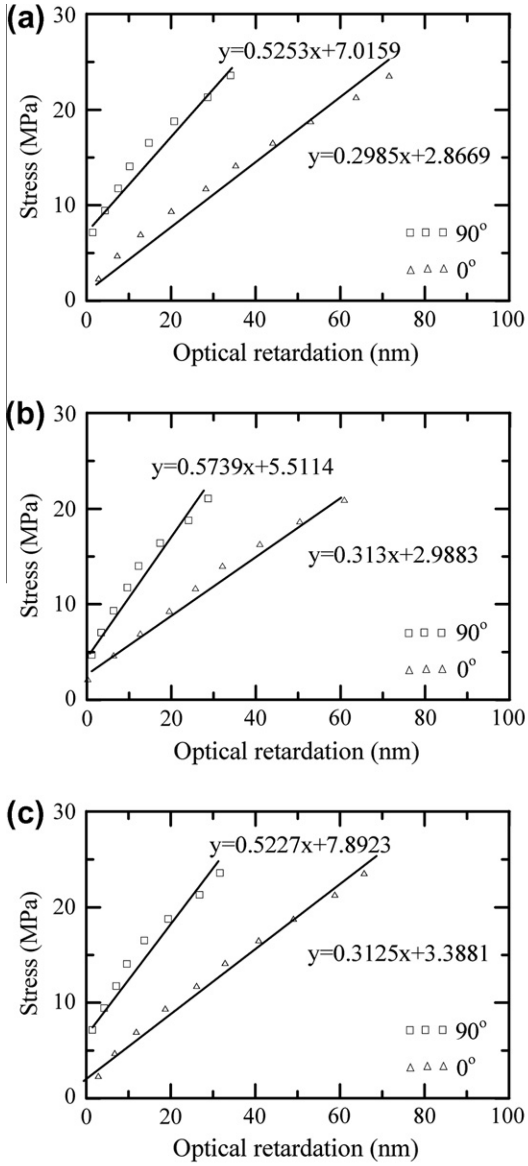

Fig. 4. Stress versus optical retardation curve for PET substrate (a) with 50 ∗ 50 pixels average under increasing tensional forces, and (b) with 50 ∗ 50 pixels average under decreasing tensional forces, and (c) with 100 ∗ 100 pixels average under increasing tensional forces.

tensional forces for PET substrates, respectively. Optical retardations of PET substrates under tensional forces in 0° and 90° orientations are also measured. A linear fit is performed on the experimental data and the stress-optical coefficient can be calculated from the slope of the equation describing the fit. The stress-optical coefficient value can be calculated from the slope and sample thickness by Eq. (1). From experimental data in Fig. 4a and b, slopes by average in 0° and 90° orientations for PET substrates at wavelength 670 nm are calculated as 0.3058 MPa/nm and 0.5496 MPa/nm, respectively. It shows that stress-optical coefficients for PET substrates in 0° and 90° orientations are different. It means that changes of optical retardations for PET substrates are different in 0° and 90° orientations under tensional stresses. In addition, data scattering can affect results but not so much due to the uniformity of a two-beam separation method. Tests for PET substrates are repeated in five times, and the standard deviation is 0.024. Fig. 4c depicts plots of stress versus optical retardation with 100 $*$ 100 pixels average under increasing tensional forces for PET substrates. By comparing Fig. 4a with Fig. 4c, it shows that trends for stress versus optical retardation curve under measured blocks of different sizes for PET substrates are close to each other. The two-beam separation method is suitable for stress-optical coefficient measurement. Fig. 5a and b depict plots of stress versus optical retardation under increasing and decreasing tensional forces for ITO-coated PET substrates. From experimental data in Fig. 5a and b, slopes in 0° and 90° orientations for ITO-coated PET substrates at wavelength 670 nm are calculated as 0.2667 MPa/nm and 0.4109 MPa/nm, respectively. It shows that stress-optic coefficients for PET substrates are smaller than that for IOT on PET substrates in 0° and 90° orientations, respectively. Therefore, optical retardations for ITO-coated PET substrates are affected more easily than that for PET substrates under tensional stress. Fig 6a and b depict plots of stress versus optical retardation under increasing and decreasing tensional forces for PEN substrates. From experimental data in Fig. 6a and b, slopes in 0° and 90° orientations for PEN substrates at wavelength 670 nm are calculated as 0.452 MPa/nm and 0.561 MPa/nm, respectively. In

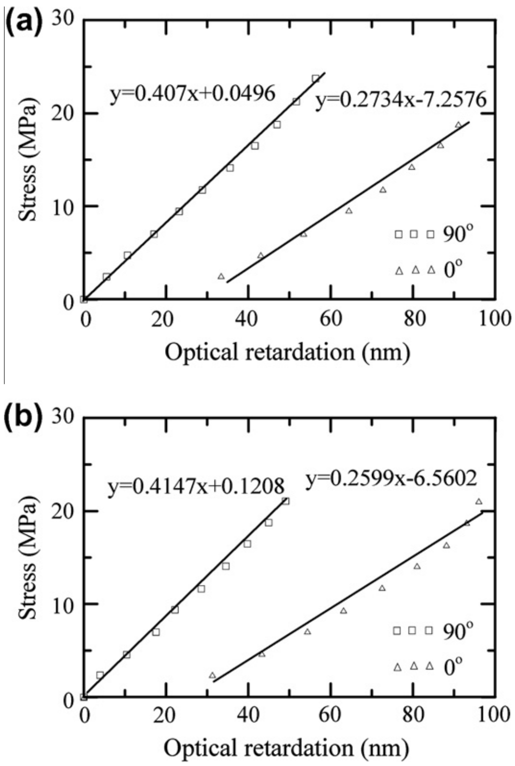

Fig. 5. Stress versus optical retardation curve under (a) increasing and (b) decreasing tensional forces for ITO-coated PET substrate.

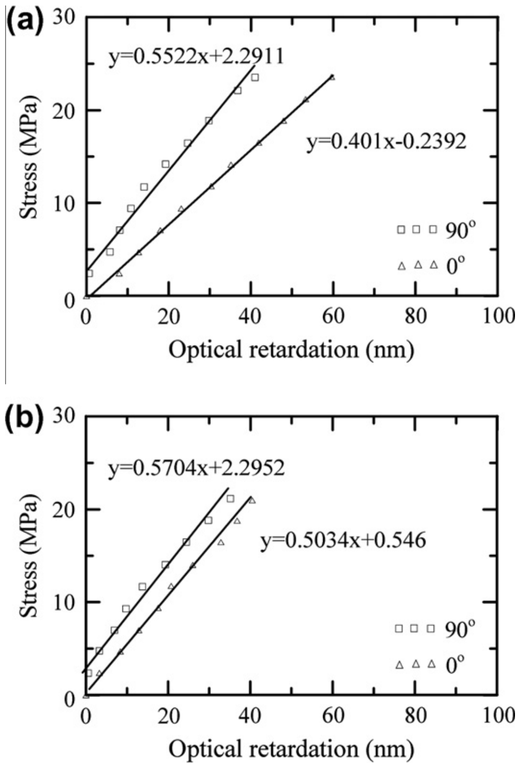

Fig. 6. Stress versus optical retardation curve under (a) increasing and (b) decreasing tensional forces for PEN substrate.

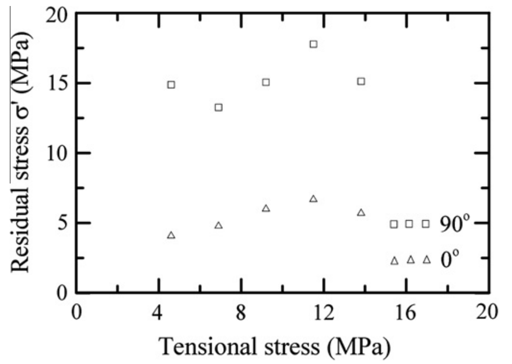

Fig. 7. Residual stress versus tensional stress curve in 0° and 90° orientations.

addition, it shows that the difference of stress-optical coefficients for PEN substrates in 0° and 90° orientations is smaller than PET substrates. As the result, the distribution of optical retardations for PEN substrates is more uniform under loading than that for PET substrates.

5. Stress measurement induced by ITO films

For stress measurement induced by ITO films, optical retardations for PET substrates and ITO-coated PET substrates under tensional stresses in 0° and 90° orientations are measured. Compared with PET substrates, ITO films is very thin. By subtracting Eq. (2) from Eq. (3), the residual stress σ' under tensional stresses can be calculated as shown in Fig. 7. It shows that stress component σ' does not affected by tensional stresses and can be regarded as the residual stress caused by ITO films. Furthermore, it shows that residual stresses σ' in 0° and 90° orientations are different. The residual stress σ' in the 0° orientation is about 10 MPa larger than that in the 90° orientation.

6. Conclusions

In this paper, a two-dimensional photoelasticity with higher measured speed and better uniformity is proposed by using a PBS connecting with two CCD cameras that are used to capture the intensity of right-hand and left-hand circular polarization separately. Stress-optical coefficients of the PET, ITO-coated PET, and PEN substrates are measured by two-dimensional photoelasticity. These samples are exerted by increasing and decreasing tensional forces and optical retardations are calculated from tensional stresses. A linear fit was performed on the experimental data and the stress optic coefficient value can be calculated from the slope describing the fit and the sample thickness. It shows that stress-optical coefficients for these substrates in 0° and 90° orientations are different. Optical retardation changes for unit tensional stress for PEN substrates in 0 an 90° orientations are smaller than PET substrates. In addition, an analytical model has been presented for residual stress caused by ITO thin film on PET substrates under tensional stresses. It shows that residual stresses for ITO-coated PET substrates are different in 0° and 90° orientations.

References

[1] M.C. Choi, Y. Kim, C.S. Ha, Polymers for flexible displays: from material selection to device applications, Prog. Polym. Sci. 33 (6) (2008) 581–630.

[2] S. Grego, J. Lewis, E. Vick, D. Temple, Development and evaluation of bend-testing techniques for flexible-display applications, J. Soc. Inf. Display 13 (7) (2005) 575–581.

[3] Y.L. Chen, H.C. Hsieh, W.T. Wu, B.J. Wen, W.Y. Chang, D.C. Su, An alternative bend-testing technique for a flexible indium tin oxide film, Displays 31 (4–5) (2010) 191–195.

[4] G.G. Stoney, The tension of metallic films deposited by electrolysis, Proc. Roy. Soc. 82 (553) (1909) 172–175.

[5] S.G. Malhotra, Z.U. Rek, S.M. Yalisove, J.C. Bilello, Analysis of thin film stress measurement techniques, Thin Solid Films 301 (1–2) (1997) 45–54.

[6] Manuel F.M. Costa, V. Teixeira, Residual stress measurement in PVD optical coatings by microtopography, Measurement 44 (3) (2011) 549–553.

[7] Z.B. Zhao, J. Hershberger, S.M. Yalisove, J.C. Bilello, Determination of residual stress in thin films: a comparative study of X-ray topography versus laser curvature method, Thin Solid Films 415 (1–2) (2002) 101–104.

[8] S. Massl, H. Kostenbauer, J. Keckes, R. Pippan, Stress measurement in thin films with the ion beam layer removal method: influence of experimental errors and parameters, Thin Solid Films 516 (23) (2008) 8655–8662.

[9] Z. Suo, E.Y. Ma, H. Gleskova, S. Wagner, Mechanics of rollable and foldable film-on foil electronics, Appl. Phys. Lett. 74 (8) (1999) 1177–1179.

[10] G.C.A.M. Janssen, M.M. Abdalla, F. Van Keulen, B.R. Pujada, B. Van Venrooy, Celebrating the 100th anniversary of the Stoney equation for film stress developments from polycrystalline steel strips to single crystal silicon wafers, Thin Solid Films 517 (6) (2009) 1858–1867.

[11] J.W. Dally, W.F. Riley, Experimental Stress Analysis, third ed., McGraw-Hill, New York, 1991.

[12] K. Ramesh, Digital Photoelasticity, Springer, Berlin, 2000.

[13] K. Ramesh, Photoelasticity Springer Handbook of Experimental Solid Mechanics, Springer, Berlin, 2006.

[14] C.W. Chang, P.H. Chen, H.S. Lien, Evaluation of residual stress in pre-stressed concrete material by digital image processing photoelastic coating and hole drilling method, Measurement 42 (4) (2009) 552–558.

[15] C.W. Chang, H.S. Lien, J.H. Lin, Determination of reflection photoelasticity fringes analysis with digital image-discrete processing, Measurement 41 (8) (2008) 862–869.

[16] S. Yoneyama, Y. Morimoto, M. Kawamura, Two-dimensional stress separation using phase-stepping interferometric photoelasticity, Measure. Sci. Technol. 16 (6) (2005) 1329–1334.

[17] R. Priestley, Birefringence dispersion in fused silica for DUV lithography, Proc. SPIE 4346, 2001, pp. 1300–1305.

[18] C.I. Wu, W.Y. Lin, C.L. Tien, Y.C. Lee, Stress measurement of ITO film on PET substrate by curvature method and polarization method, Organic Semiconductor Conference & Exhibition, London UK, 2009.